PROCEEDINGS OF SPIE

SPIEDigitalLibrary.org/conference-proceedings-of-spie

Prototype of meta-surface anti-reflection coating for a 40GHz HDPE lens

Lu, Xuefeng, Li, Zhengwei, Liu, Congzhan, Zhang, Yifei, Xu, Yu, et al.

Xuefeng Lu, Zhengwei Li, Congzhan Liu, Yifei Zhang, Yu Xu, Guanhua Gao, Zhao Feng, Guofu Liao, Xufang Li, Yudong Gu, Laiyu Zhang, "Prototype of meta-surface anti-reflection coating for a 40GHz HDPE lens," Proc. SPIE 12072, 10th International Symposium on Advanced Optical Manufacturing and Testing Technologies: Micro- and Nano-Optics, Catenary Optics, and Subwavelength Electromagnetics, 120720B (13 December 2021); doi: 10.1117/12.2604929

Event: Tenth International Symposium on Advanced Optical Manufacturing and Testing Technologies (AOMATT 2021), 2021, Chengdu, China

Prototype of meta-surface anti-reflection coating for a 40GHz HDPE lens

Xuefeng Lu[a], Zhengwei Li[a], Congzhan Liu*[a], Yifei Zhang[a], Yu Xu[a], Guanhua Gao[a], Zhao Feng[a], Guofu Liao[a], Xufang Li[a], Yudong Gu[a], Laiyu Zhang[a]
[a]Institute of High Energy Physics Chinese Academy of Sciences, Beijing, China 100049

ABSTRACT

For cosmic microwave background (CMB) telescopes, high-density polyethylene (HDPE) is widely used as reimaging lens material on account of its extremely low loss and excellent mechanical properties. The impedance mismatch between free space and lens can cause non-negligible reflection loss and low image quality. An anti-reflection (AR) coating is essential to reduce such effect. Single or multiple layers porous polytetrafluoroethylene (PTFE) membranes are glued to the HDPE lens surface as AR coatings in many previous CMB experiments. However, it is difficult to get a uniform bonding across a curvature surface for a large-aperture CMB telescope. Due to the mismatch of the thermal expansion of the lens and AR coating materials, the AR coatings have delamination or separation problem during cryogenic cycling. Simulated dielectric AR (SDAR) coatings based on the theory of meta-surface are suitable for low frequency and large aperture CMB telescopes. The effective refractive index of SDAR coating is tunable by cutting holes or grooves into the lens material to form sub-wavelength structure. The SDAR coating is made directly from lens bulk material, which can naturally solve the thermal expansion mismatch problem. In this paper, we present the SDAR coating prototype machined on a 30 mm thick HDPE plate. The measurement results show that the SDAR coating can effectively eliminate standing waves with the performance improvement about -10 dB to -20 dB. And the transmittance exceeds 98% in the 30 GHz to 50 GHz band, which is about 10% higher than that without AR coating.

Keywords: CMB, telescope, HDPE, anti-reflection coating, simulated dielectric, 40 GHz, cross polarization, meta-material

1. INTRODUCTION

Primordial gravitational waves (PGW) originates from space-time perturbation in the Big Bang. The detection of PWG is the most direct and effective way to explore the universe origin and evolution, such as the inflation theory, the bouncing cosmology, and the cyclical universe. And it becomes a fundamental physics core issues such as for Charge, Parity, and Time reversal symmetry test. The wavelengths of primordial gravitational waves are comparable to the size of the universe. It can only be detected by measuring the B-mode polarization of the CMB. The B-mode CMB polarization signal is extremely weak and contaminated easily by the foreground radiation of the Milky Way. For the B mode polarization, the foreground is dominated by synchrotron radiation in low frequency and thermal dust radiation in high frequency.

To accurately measure CMB B mode polarization, the foreground contamination must be removed first. Due to the existence of atmosphere, the observable windows for on-ground CMB experiments are mainly concentrated at 40 GHz, 95 GHz, 150 GHz and 220 GHz. At low frequency, such as the 40 GHz band, synchrotron radiation dominates the foreground contamination. The measurement in this frequency band can be used to deduce the foreground synchrotron radiation. Almost all the CMB polarization experiments employ cold refraction lenses system. As impedance mismatch, reflections on dielectrics boundaries can cause energy loss and systematic errors[1]. HDPE has lower cost and extremely low loss in millimeter and sub-millimeter wave bands, its good mechanical properties made processing and shaping much easier than silicon and alumina. As commonly used HDPE plastic lenses, have a reflection loss up to 10% for a single lens, which is 50% for silicon and alumina lenses. Anti-reflection coatings is critically needed to eliminate such effect for improving sensitivity of the CMB telescope.

Usually there are two types of anti-reflection coatings, quarter-wavelength coatings for narrow band and gradient index coatings for broad band[2]. The traditional quarter-wavelength anti-reflection coating is to bond appropriate refractive index (n_{AR} = square root (n_{sub})) material to the lens surface. However, due to the scarcity of millimeter-wave low-loss materials, it is difficult to find proper anti-reflection coating materials which exactly match the required refractive index.

AOMATT 2021: Micro- and Nano-Optics, Catenary Optics, and Subwavelength Electromagnetics,
edited by Mingbo Pu, Xiong Li, Xiaoliang Ma, Minghui Hong, Emmanuel Stratakis, Xiangang Luo,
Proc. of SPIE Vol. 12072, 120720B © 2021 SPIE · 0277-786X · doi: 10.1117/12.2604929

The bonding layer will delaminate and separate from the lens surface as the thermal expansion difference between the lens and coating layer at cryogenic temperature. The metasurface uses different topographies to control the boundary conditions of the electromagnetic wave[3], thus changing the characterized equivalent dielectric constant of the medium. Therefore, it is widely used in structural optics[4] and lens antenna[5] and antireflection coatings. The refractive index of artificial dielectric layer[6] can be tuned by adding sub-wavelength structures, such as holes, grooves or compound eyes. The sub-wavelength structures on the surface of the material is used to form air gaps, which has similar properties as This kind AR coating has excellent performance. For example, any index between *n* and 1 can be achieved and has high stability at low temperature and insensitivity to polarization. SDAR coating for HDPE lens have been used in CAPMAP[7] and CLASS[8] with square array of holes.

2. SIMULATED DIELECTRIC ANTI-REFLECTION LAYER THEORY AND DESIGN

2.1 Simulated dielectric layer theory

For simulated dielectric anti-reflection coating, the equivalent dielectric constant of the interface is adjusted by cutting the air gap structure into the bulk material surface. The dielectric constant depends on the area ratio of the openings. For machining convenience and getting low cross polarization, we modeled the structure with square array of holes, the equivalent circuit is shown in Figure 1. Dividing up the unit cell into several capacitors, it is equivalent to a series and parallel circuit. The equivalent dielectric constant of the anti-reflection coating can be expressed as equation (1) to (3) [6], *C* is capacitance, which equals to the product of dielectric constant and thickness. The blank is air whose dielectric constant ϵ_0 is about 1, while the left is substrate with ϵ_r is larger than air, *d* is the thickness of the SDAR layer, *a* is the grid period, and *b* is the diameter of the opening. The simulation model assumes parallel electric fields within the unit cell. The solved total capacitance divided by thickness and vacuum dielectric constant to get the theoretical relative dielectric constant of the antireflection coating.

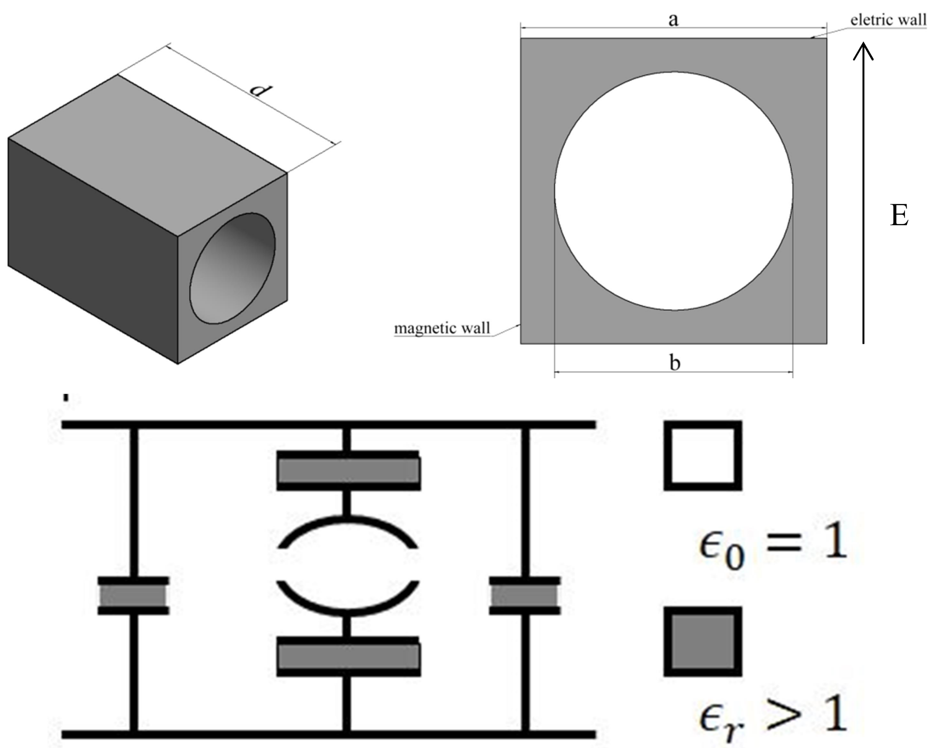

Figure 1. Equivalent circuit of the simulated dielectric structure, the blank is air whose dielectric constant ϵ_0 is about 1, while the left is substrate with ϵ_r is larger than air, *d* is the thickness of the SDAR layer, *a* is the grid period, and *b* is the diameter of the opening. The simulation model assumes parallel electric fields within the unit cell, for different part dividing up the unit cell into several capacitors[3]. The arrow indicates the direction of the electric field.

$$C = \epsilon_0 \varepsilon \epsilon_r \frac{(a-b)d}{a} + \int_{\frac{-b}{2}}^{\frac{b}{2}} \frac{\epsilon_0 \epsilon_r d}{a + y_B(x)(2\epsilon_r - 2)} dx \quad (1)$$

$$y_B(x) = \sqrt{\left(\frac{b}{2}\right)^2 - x^2} \quad (2)$$

$$\epsilon_r^{eff} = \frac{C}{d\epsilon_0} \quad (3)$$

We define duty cycle as:

$$r = \frac{b}{a}$$

For our 40 GHz CMB telescope prototype, HDPE is adopted as lens material. The high density polyethylene material is from Dezhou Xinxu Wear Resistant Co. Ltd. The measured dielectric constant and loss tangent of the HDPE is shown in Figure 2, which are consistent with that of the referenced results[9]. Based on the above equations we get a relationship curve between effective dielectric constant and the duty cycle *r* is shown in Figure 3. The dielectric constant of HDPE is about 2.36@40 GHz, and the required dielectric constant of the anti-reflection coating is 1.536 based on equation (4) and (5)[1]. According to the calculation result in Figure 3, 1.536 give the corresponding duty cycle *r* is 0.78.

$$n = \sqrt{\varepsilon_r * \mu_r} \quad (4)$$

$$n_{AR} = \sqrt{n_{HDPE}} \quad (5)$$

here *n* is refractive index, ε_r is the relative dielectric constant and μ_r is the relative permeability, $\mu_r \approx 1$. n_{AR} is the needed refractive index of AR coating, n_{HDPE} is the refractive index of substrate material.

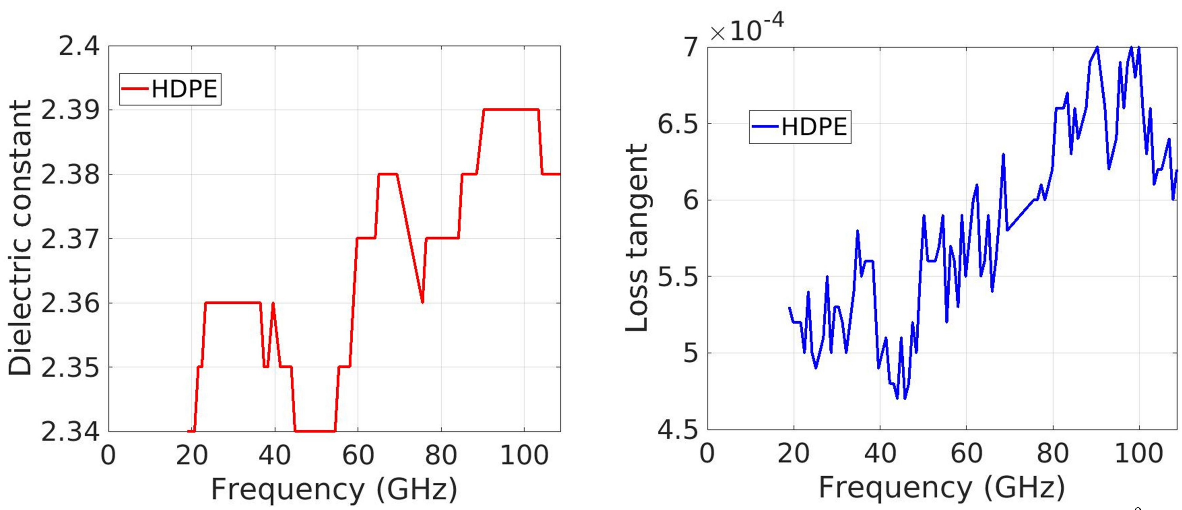

Figure 2. Measured dielectric constant (left) and loss tangent (right) of HDPE, which are consist with the reference [9] data

2.2 SDAR design for HDPE

The center frequency of the planned CMB telescope prototype is 40 GHz, combining the best adaptive bandwidth of a quarter wave SDAR and observation requirements, 50% of the bandwidth is selected, which means 30 GHz to 50 GHz. According to the conditions mentioned in the literature[10], when the pitch of the grid of the anti-reflection coating is close to the wavelength, high-order diffraction effect is likely to occur. The condition for first-order diffraction is defined as:

$$\lambda = \delta \times n_{substrate} \quad (6)$$

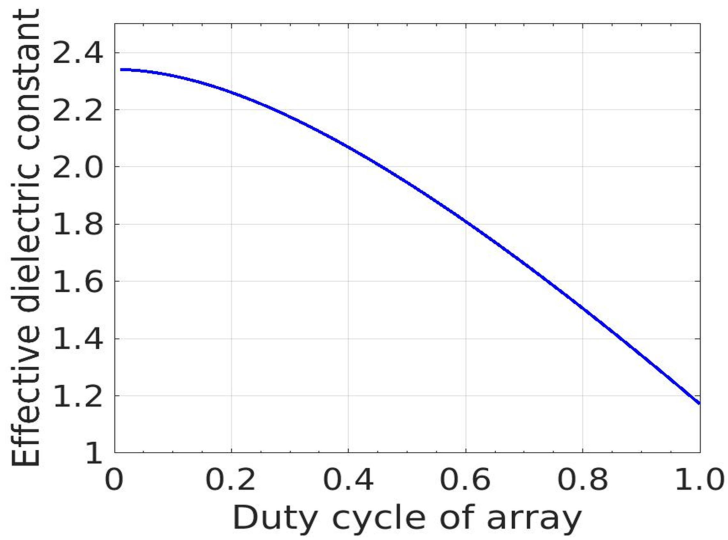

Figure 3. Gap ratio versus equivalent dielectric constant for cylindrical holes, thickness d is independent of the equivalent permittivity

In equation (4) λ is the wavelength, δ is the pitch of the grid, and $n_{substrate}$ is the material refractive index.

The refractive index of HDPE n_{PE} is 1.536, the minimum wavelength during the bandwidth is about 6 mm, based on formula (4) the pitch of the grid δ needs to be less than 3.9 mm.

The equivalent refractive index of the anti-reflection coating required by HDPE is n_{AR} = square root (n_{PE}) = 1.239. Starting from the central frequency of 40 GHz (means wavelength ~7.5 mm), the thickness needed for the anti-reflection coating is $h = \lambda/(4n_{\mathrm{AR}}) = 1.51$ mm.

Based on HFSS[14] software, different grid period of the array between 0.5 mm and 4.0 mm was simulated, as shown in Figure 4, when the period less than 1.2 mm, the S11 parameter remains at the same low level. A period of 1 mm was chosen to give an easy position control for machining.

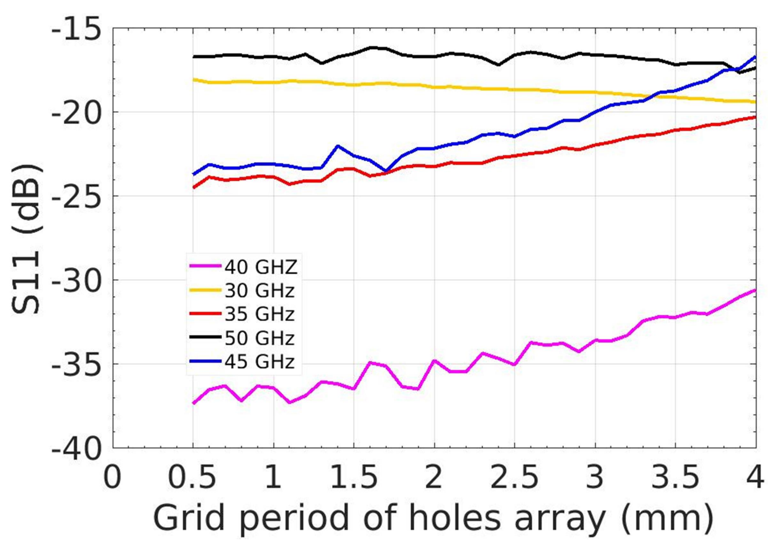

Figure 4. S11 vary with grid period of holes array, the curve from bottom to top are simulated result at 40 GHz, 35GHz, 45GHz, 30GHz and 50 GHz respectively. Hole diameter equals 0.78 multiply period.

The designed parameters were used in HFSS[14] modal, as shown in Figure 5, the blue line shows that the simulated transmittance of the entire frequency band is above 98%. Compared with that without anti-reflection coating (the black dash line in Figure 5), the transmittance is significantly improved and the standing wave is perfectly eliminated.

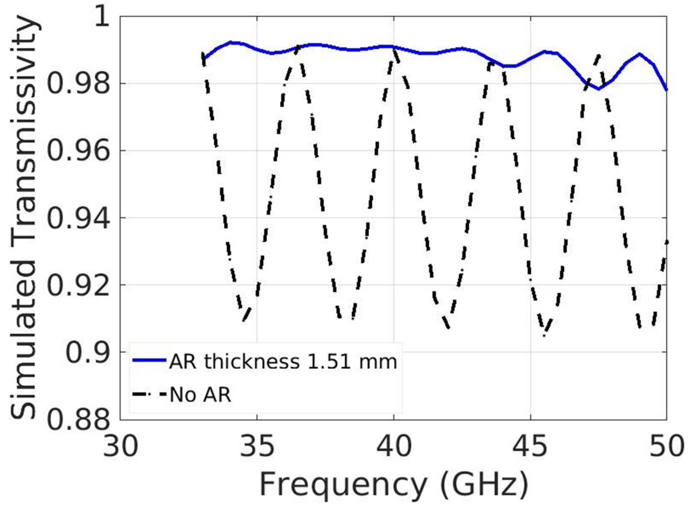

Figure 5. Simulated Transmittance at different frequency. The blue line is the simulated Transmittance for HDPE with 1.51 mm thick AR coating. The gap ratio and grid period of the AR are 0.78 and 1 mm respectively. The black dash line is the simulated transmissitvity without AR.

3. PROTOTYPE OF ANTI-REFLECTION COATING

3.1 Mechanical properties of simulated Dielectric anti-reflection coating

Because HDPE is easier to process, mechanical or laser can usually be chosen to complete the design of anti-reflection coating processing. However, considering the need to cut holes on the surface of the lens with curvature in practice, laser processing needs to develop special equipment, which costs a lot. In this study, the method of mechanical processing is selected. Firstly, a 30 mm thick with size 300 mm*300 mm slab is machined, the surface is polished, and the residual stress of mechanical processing is released by annealing treatment. Then, AR array is drilled by Computer Numerical Control (CNC) machine tool with a 0.78 mm alloy drill bit and water cooling method. It should be noted that HDPE material is soft, and the bit speed is should higher to keep holes fineness, but too high speed is easy to melt the material. After several attempts, 2500 rpm was used in this experiment. The roundness of the machined holes was checked by white light surface profilometer. As shown in Figure 7, circular holes are evenly arranged and the roundness meets the design requirements. The blind hole's depth of the sample was measured by ThinkFocus confocal 3D profilometer SM-5000. The results are shown in Figure 6, the measured real depth is about 1.77 mm, which is deeper than design value 1.51mm. CNC drilling can better control the error in depth, while design and machine forget to consider the front end of the drill bit has a 118° cone angle structure, shown in Figure 8, the influence on S parameter is discussed in the next section.

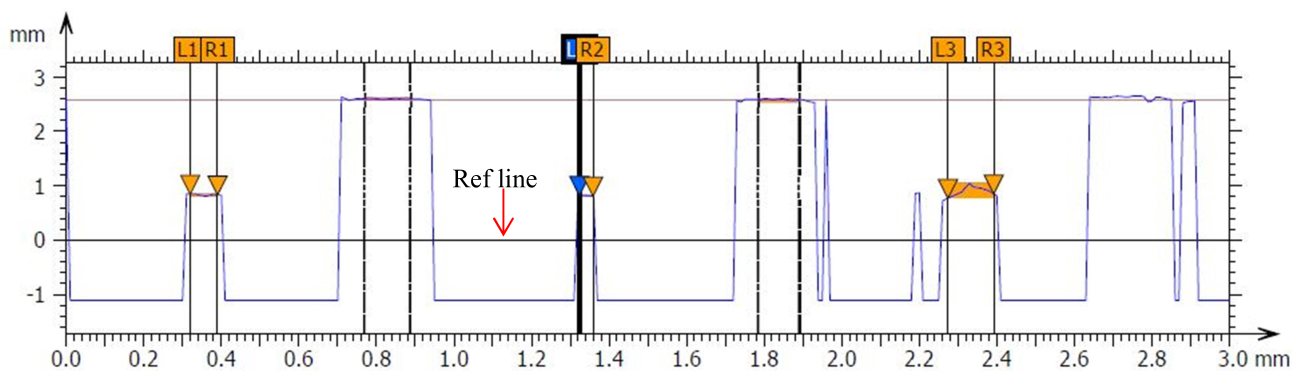

Figure 6 . Test result of hole depth with confocal 3D profilometer, the average value for each L1R1 is 1.763 mm, L2R2 1.777 mm, L3R3 1.695 mm, for L3R3 the fluctuation is big which means a not accurate value.

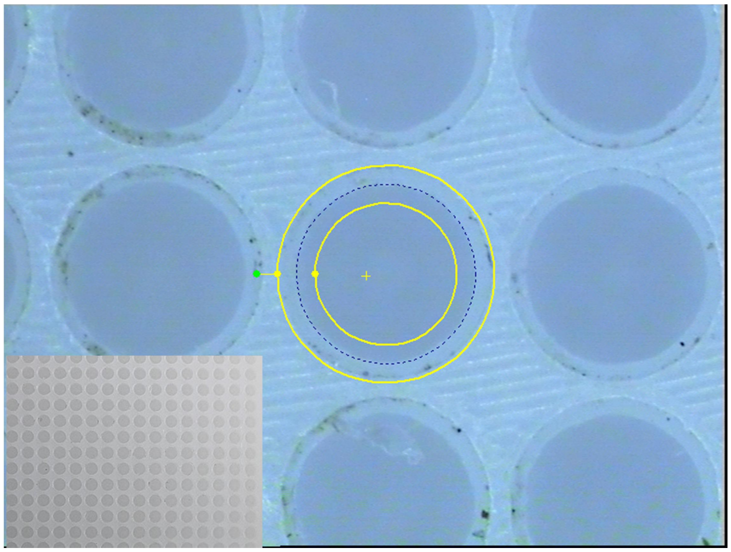

Figure 7. Measured surface profile of SDAR layer with white light profilometer. The measured grid pitch is 1 mm, hole diameter is 0.78 mm. The image in the left bottom corner of the figure is the real photo of the AR coating.

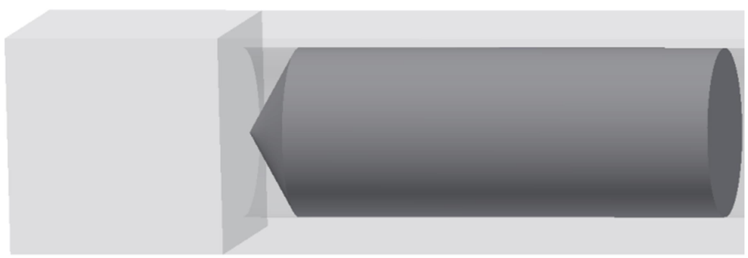

Figure 8. Drill bit cone structure, with diameter 0.78 mm, cone angle 118 degrees, light grey is the HPDE material and dark grey is the drill bit shape with material vacuum, the model is used for analysis in HFSS[14]

3.2 Test system

The free space method is suitable for non-contact measurement of high frequency transmission parameters, and the sample needs to be planar and large enough to reduce the influence of edge diffraction effect. According to the test method described in literature[11], the RCHO22R horn antennas were selected as transmitter and receiver of the free space test system, and the vector network analyzer Agilent E8361A was used as the excitation source to test the S parameters of the sample from 33 GHz to 50 GHz. The test system was calibrated both with GRL[12] and TRL[13] calibration method, when the more accurate TRL calibration method was finally adopted to complete the test. The system is arranged within the Rayleigh distance of the antenna to reduce the sample size as much as possible. Antenna spacing: 225 mm (~ 30 λ_0, λ_0=7.5 mm), spot size in the middle position: 7 λ_0, sample size: 300 mm × 300 mm which is three times than the spot size. The free space system is shown in the Figure 9. The antenna alignment accuracy is guaranteed by the clamping structure. At the beginning of the sample test, the metal plate reflection test can be used to center the sample fixture.

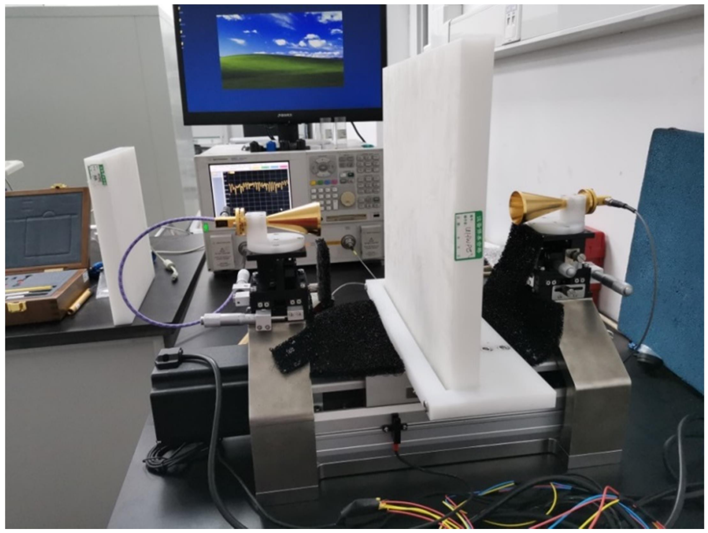

Figure 9 Diagram of free space test system, the two horn antennas are co-polarized and aligned by the two 3D moveable tools.

3.3 Test result

The AR coating designed for 40 GHz choose cylinder holes with 1 mm grid period, 1.51 mm thick and 0.78 duty circle. As shown in Figure 10, the red line is the measured transmittance of HDPE with a SDAR coating, the value is better than 98% between 33 GHz and 50 GHz. The standing wave shown in the red dot line which have no AR coating is completely eliminated.

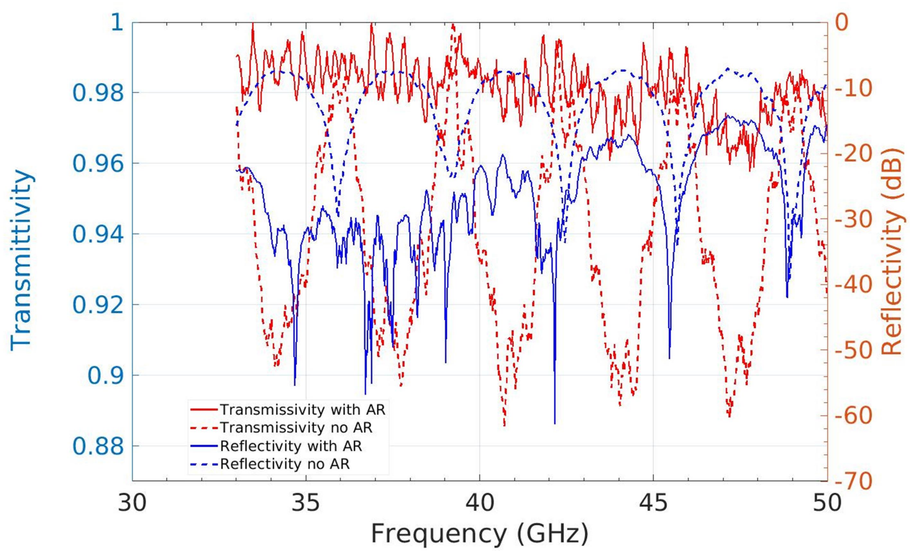

Figure 10 Measured S11 parameter and transmittance of HDPE with and without coating, red line: transmittance with AR coating, red dot line: transmittance without AR coating, blue line: reflectivity with AR coating, blue dot line: reflectivity without AR coating.

3.4 Discussion

Figure 11 shows the test and simulation results for HDPE with a simulated dielectric antireflection coating. It is found that the measured transmittance is lower than that of the simulation. The main reasons may include:

First, The location precision of the transmitting antenna and the receiving antenna is ensured by the mechanical design of the fixture， that the two antennas may not absolutely co-polar and coaxial due to the influence of fabrication tolerances;

Second, the cutting process introduced errors to the actual hole size. The fabrication accuracy of the drill bit is introduced into the HFSS model to evaluate the effect of the fabrication process. The simulated result is shown by the black short dash line in Figure 11. It is found that the simulated result with fabrication accuracy is more consistent with the measured result.

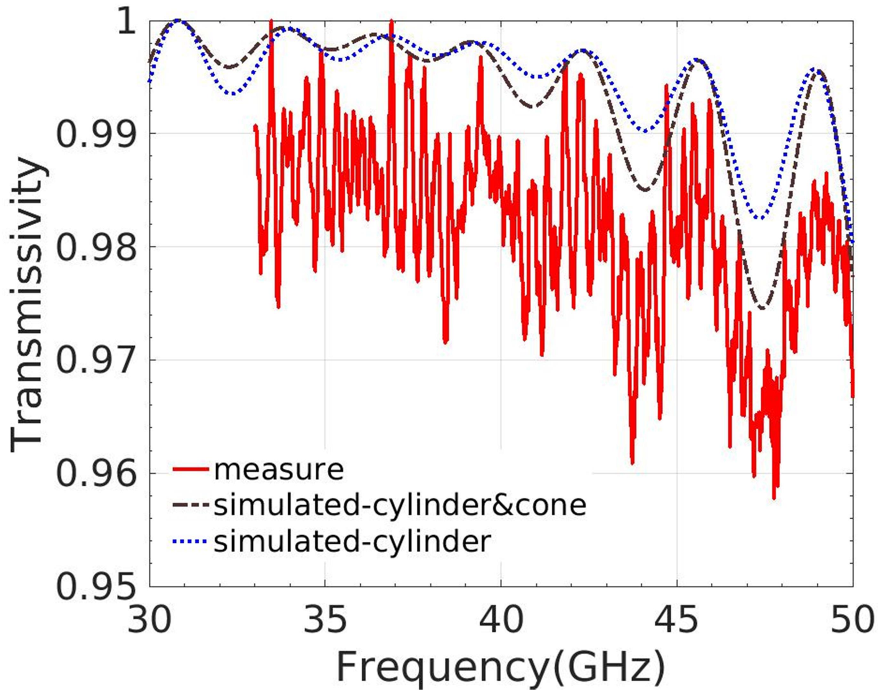

Figure 11 Transmittance of HDPE with AR coating, red solid line: measured data; blue dot line: simulated data with cylinder, black dash line: simulated data with modified model which take consideration of the cone structure at the bottom of the hole.

4. CONCLUSION

In this work, we design and fabricated a simulated dielectric anti-reflection (SDAR) coating prototype by machined on a 30 mm thick high-density polyethylene (HDPE) plate. And the measurement results show that the SDAR coating can effectively eliminate standing waves with a performance improvement about -10 dB to -20 dB. Besides the transmittance exceeds 98% in the 30 GHz to 50 GHz band, with about 10% increase than that without anti-reflection (AR) coating, the standing wave has also been eliminated effectively. In the optical system of CMB telescope, the lens works at 4 K or lower temperature environment, it is necessary to consider the impact of shrinkage, leaving enough margin to ensure that the performance meets the requirements at low temperature.

REFERENCES

[1] Hargrave, P. C. & Savini, G., "Anti-reflection coating of large-format lenses for sub-mm applications," *Proc. SPIE* **7741**, 77410S-77410S–10 (2010).

[2] Mcmahon, J, "Simulated Dielectric Anti- Reflection Coatings," University of Chicago.

[3] Luo, X. G., "Principles of electromagnetic waves in metasurfaces," *Sci. China Physics, Mech. Astron.* 58, 1–18 (2015).

[4] Guo, Y. et al., "High-Efficiency and Wide-Angle Beam Steering Based on Catenary Optical Fields in Ultrathin Metalens," *Adv. Opt. Mater.* 6, 1800592 (2018).

[5] Yang, J., Zeng, Y., Jin, S., Wen, C. K. & Xu, P., "Communication and Localization with Extremely Large Lens Antenna Array," *IEEE Trans. Wirel. Commun.* 20, 3031–3048 (2021).

[6] Biber, S., Richter, J., Martius, S. & Schmidt, L. P., "Design of artificial dielectrics for anti-reflection-coatings," *Conf. Proc. - 33rd Eur. Microw. Conf. EuMC 2003* **3**, 1115–1118 (2003).
[7] Jeff, M^{c}. Mahon., "THE 2004-2005 CAPMAP INSTRUMENT AND CMB POLARIZATION DATA (2006)," Princeton University PhD thesis. 2006.
[8] Harrington, K. M., "Variable-delay Polarization Modulators for the CLASS Telescopes," PhD thesis, A dissertation submitted to The Johns Hopkins University. (2018).
[9] Lamb, J. W., "Miscellaneous data on materials for millimetre and submillimetre optics," (2015). doi:10.1007/BF02069487
[10] Chen, Y. W. & Zhang, X., "Anti-reflection implementations for terahertz waves," 1–20 (2013). doi:10.1007/s12200-013-0377-z
[11] Hassan, A. M., Obrzut, J. & Garboczi, E. J., "A Q-Band Free-Space Characterization of Carbon Nanotube Composites," *IEEE Trans. Microw. Theory Tech.* **64**, 3807–3819 (2016).
[12] Du Liuge , Hu Dahai , Zhao Rui, W. Y, "A modified time-domain gating calibration method for free-space material measurement," *2015 IEEE 12th Int. Conf. Electron. Meas. Instruments* 613–616 (2015).
[13] Rolfes, I. & Schiek, B, "Calibration methods for microwave free space measurements," *Adv. Radio Sci.* **2**, 19–25 (2004).
[14] ELECTROMAGNETIC IMULATION OFTWARE, 3D Electromagnetic Field Simulator for RF and Wireless Design, https://www.ansys.com/zh-cn/products/electronics/ansys-hfss